JOURNAL OF GEOPHYSICAL RESEARCH, VOL. 106, NO. A12, PAGES 30,331–30,336, DECEMBER 1, 2001

Observations of equatorial *F* region plasma bubbles using simultaneous OI 777.4 nm and OI 630.0 nm imaging: New results

J. R. Abalde and P. R. Fagundes
Instituto de Pesquisas e Desenvolvimento, Universidade do Vale do Paraíba, São José dos Campos - SP, Brazil

J. A. Bittencourt and Y. Sahai
Instituto Nacional de Pesquisas Espaciais, São Paulo, Brazil

Abstract. Simultaneous observations of the OI 630.0 nm and OI 777.4 nm nightglow emissions using all-sky imaging systems and ionospheric radio sounding using a Canadian Advanced Digital Ionosonde (CADI) digisonde have been recently carried out at São José dos Campos (23.21°S, 45.86°W), Brazil. The all-sky imaging systems use novel CCD devices, with high quantum efficiency and which provide an exceptional capacity for quantitative measurement of faint- and low-contrast emissions. On October 23-24, 2000 (high solar activity), the presence of large-scale *F* region plasma irregularities (plasma bubbles) was observed using both techniques (i.e., optical and radio). The high-resolution images, recorded using the OI 777.4 nm nightglow emission, show a new striated or ray-like pattern, which has not been detected before. These OI 777.4 nm optical observations show for the first time, in great detail, the field-aligned ionospheric plasma bubble structures, in contrast with the OI 630.0 nm images, which show a diffuse image of the bubbles. The optical signatures of the OI 777.4 nm emission are more closely related to the actual ionospheric bubble structure, owing to its prompt emission and dependence only on the electron density, with no *F* layer height dependence. On the other hand, the OI 630.0 nm emission comes from the bottomside of the *F* layer with a strong *F* layer height dependence and shows blurred images due to its 110-s lifetime. An additional advantage of using the OI 777.4 nm emission for ionospheric irregularity studies is that the plasma bubbles can be observed earlier on the OI 777.4 nm images than on the OI 630.0 nm images (by ~ 15 min).

1. Introduction

The novel CCD devices used in our upper atmosphere optical experiments nowadays provide an optical image of atomic and/or molecular nightglow emissions with much higher temporal and spatial resolution than that achieved in recent years. The nightglow emissions are usually very faint and sometimes may present spatial and temporal fluctuations of a few percent, which can be attributed to the propagation of waves or to spatial irregularities in the upper atmosphere [Garcia et al., 1997]. In August 2000, optical and ionospheric radio measurements for ionospheric and thermospheric studies were started at São José dos Campos (23.21°S, 45.86°W), Brazil, using two all-sky imaging photometers and a Canadian Advanced Digital Ionosonde (CADI) digisonde. Large-scale ionospheric irregularity studies are our primary aim during the present solar maximum period, since occurrences of plasma bubbles, with some of them attaining very high altitudes (>1500 km) at the magnetic equator, are more frequent during high solar activity [*Sahai et al.*, 1999, 2000]. Also, the ionospheric conditions for the generation and growth of plasma bubbles have been studied by many investigators [*Ossakow*, 1981; *Kelley*, 1985; *Mendillo et al.*, 1992]. There is a general agreement that the rapid postsunset **E x B** upward plasma drift of the *F* layer, which is one of the important conditions for the onset of ionospheric irregularities, occurs more frequently during high solar activity.

Paper number 2001JA001115.
0148-0227/01/2001JA001115$09.00

Large-scale equatorial ionospheric irregularities have been extensively studied by means of the OI 630 nm nightglow emission imaging during the last three decades [*Weber et al.*, 1978; *Mendillo and Baumgardner*, 1982; *Sahai et al.*, 1994, 1999, 2000; *Fagundes et al.*, 1999; *Sinha and Raizada*, 2000]. The OI 630.0 nm emission comes from the *F* layer bottomside (240 - 300 km) and is produced by the dissociative recombination process $O_2^+ + e \rightarrow O^* (^1D)$, $O^* \rightarrow O(^3P) + h\nu$ (630.0 nm), where the metastable $O(^1D)$ has a radiative lifetime of 110 s. The OI 630.0 nm emission intensity is proportional to the column integral of the product of the $n(O_2^+)$ and $n(e)$ concentrations and is strongly affected by the *F* layer vertical motions. When the *F* layer moves upward or downward, the OI 630.0 nm emission is reduced or enhanced, respectively, thus showing an inverse dependence with the *F* layer vertical motions.

The OI 777.4 nm emission has also been used for large-scale ionospheric irregularity studies [*Moore and Weber*,

Table 1. Interference Filter Characteristics and Exposure Times for the CCD Optical Imager

Wavelength, nm	Diameter, inches	Bandwidth, nm	Transmission, %	Integration Time, s
630.0	3	2.0	84	60
777.4	3	1.5	84	60

1981; *Sahai et al.*, 1981; *Bittencourt et al.*, 1983; *Mendillo et al.*, 1985; *Rohrbaugh et al.*, 1989; *Tinsley et al.*, 1997] but not so frequently, mainly because its intensity is weaker than the OI 630.0 nm intensity and it is very small (a few rayleighs (R)) during low solar activity. The OI 777.4 nm emission is prompt and is produced mainly by the radiative recombination of O^+ [*Tinsley and Bittencourt*, 1975], according to the reaction $O^+ + e \rightarrow O\,(^5P)$, $O(^5P) \rightarrow O(^5S) + h\nu$ (777.4 nm). Its intensity is proportional to the column integral of the product of the $n(O^+)$ and $n(e)$ concentrations.

The OI 630.0 nm and OI 777.4 nm nightglow intensity depletion bands (quasi north-south aligned) observed at equatorial and low-latitude regions are the optical signatures of large-scale ionospheric irregularities, as seen in the height range of the nightglow emissions. Imaging both the emissions, using all-sky photometers with the new generation of CCD devices, the dynamics and morphology of the *F* region irregularities, in particular as shown by the high-resolution OI 777.4 nm images, can be better studied and understood. Observations from two different *F* region heights, i.e., from the bottomside (OI 630.0 nm emission) and from around the F_2 peak height (OI 777.4 nm emission), can be used to monitor the generation, evolution, and dynamics of the plasma bubbles.

In this paper we present and discuss the advantages of high-resolution simultaneous observations of OI 630.0 nm and OI 777.4 nm emissions in large-scale ionospheric irregularity studies. The OI 777.4 nm images recorded show sharp quasi north-south magnetic field-aligned structures in the plasma irregularities, which are not revealed by the OI 630.0 nm images. Also, the large-scale plasma irregularities appear first in the early evening OI 777.4 nm images.

2. The All Sky Imaging Systems

Two monochromatic imaging systems (Keo Consultants) had their initial operational tests in July 2000. They utilize a bare (back-illuminated, 1024x1024 pixel) charge-coupled device (CCD) CH350 Photometrics of high quantum efficiency (≈ 80 % in the visible). The large dynamic range and low noise characteristics (dark current < 0.5 e pixel^{-1} s^{-1}) of this device provide an exceptional capacity for quantitative measurement of faint, low-contrast (< 5 %) airglow emission variations. The camera uses a fast (*f*/4) all-sky (180°) Mamiya 24-mm telecentric lens system with a single interference filter.

Two emissions were measured (one in each imaging system) during test observations in October 2000: OI 630.0 nm and OI 777.4 nm. The exceptional sensibility of the optical imagers enabled sequential measurements at high repetition rates (one picture each 80 s with 1 min of integration time). Table 1 lists the filter characteristics and exposure times.

3. The Digital Ionosonde

A new digital ionosonde of the type known as Canadian Advanced Digital Ionosonde (CADI) [*MacDougall et al.*, 1997] was installed in August 2000 at São José dos Campos. This instrument operates from 1 to 20 MHz at vertical incidence and covers an altitude range between 90 and 1000 km. The transmitter power is 600 W, and 40 pulses per second are normally transmitted. Either an unmodulated 40-μs pulse or a 40-μs baud, 13-bit Barker coded pulse may be used. In the latter sequence the output is 13x40 μs = 520 μs long, and the 13 chips are phase coded by ± 90° in a special way. The Barker code gives an 11-dB improvement in the signal-to-noise (S/N) ratio but limits the lowest height from which echoes may be obtained.

The ionosonde antenna is a double delta dipole array supported by a 20-m tower. Coherent pulse averaging is used to further improve the S/N ratio; in practice, four pulse averages are used, giving a 6-dB S/N improvement. One of the dual antennas is used for transmitting, and the other is used for receiving. The sampling rate is 20 μs, and the altitude resolution is 6 km. The received pulses may be coherently averaged to give an additional increase in the S/N ratio proportional to the number of pulses averaged. Fast Fourier transform (FFT) processing may be used to remove the linear portion of the phase drift, when the ionosphere is sufficiently non-stationary; otherwise, phase coherence would be lost during averaging.

4. Observations

Simultaneous ionospheric sounding and OI 630.0 nm and OI 777.4 nm all-sky imaging measurements were made from

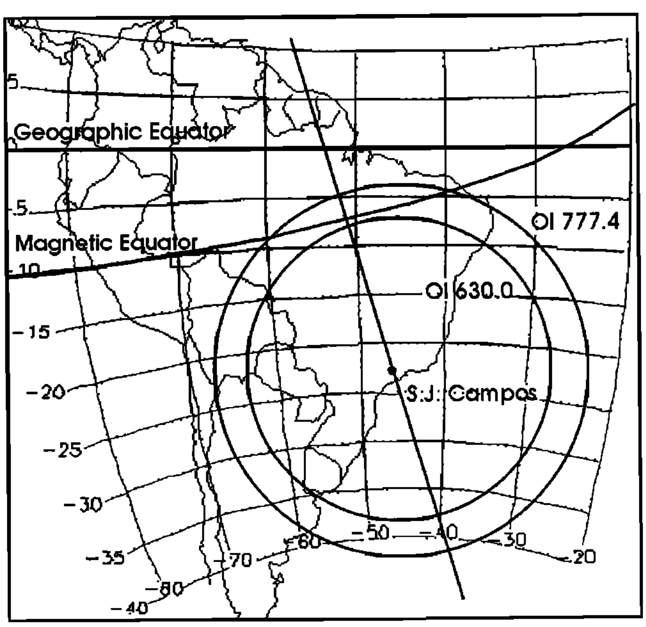

Figure 1. All-sky imaging system field of view at 90° zenith angle for the OI 777.4 nm emission (350 km of height) and for the OI 630.0 nm emission (280 km of height), as seen from the observation site of São José dos Campos. The geomagnetic equator and the magnetic north-south direction are also indicated.

the Campus of Paraíba Valley University (UNIVAP) at São José dos Campos, Brazil, from October 22 to October 24, 2000. The intensities of the OI 630.0 nm and OI 777.4 nm emission lines were imaged using two monochromatic imaging systems, one for each line. These two all-sky imaging systems cover a large area of the sky, as indicated in the map shown in Figure 1. The circles define the area of the sky as seen for a field of view of 90^o zenith angle and at 350 km of height for the OI 777.4 nm emission and at 280 km of height for the OI 630.0 nm emission. The magnetic north direction at São José dos Campos (located at ~ 16^o dip latitude) is also shown in Figure 1. Images were obtained every 80 s, with an integration time of 60 s on each night for both imaging systems, and recorded on the hard disk of a computer.

For comparison, a sample of the OI 630.0 nm and OI 777.4 nm all-sky images are presented in Figure 2, showing different patterns in their airglow depletion structures. Figure 3 presents two sequences of the OI 777.4 nm and OI 630.0 nm all-sky images for the night of October 23, 2000, showing the time evolution and spatial characteristics of large-scale plasma irregularities, as seen from each emission. Note, in Figures 2 and 3, that the pictures have a dark area in their lower portion, resulting from the use of shades to block artificial lights from nearby cities. During the course of the observations we detected a high-resolution, ray-like, fine structure pattern in the OI 777.4 nm images, associated with large-scale ionospheric plasma irregularities.

The digital ionosonde measures, on a routine basis, one ionospheric profile at every 5 min. The observed ionospheric parameters $h'F$ and f_oF_2 are shown in Figure 4, for the nights of October 22-23, 23-24, and 24-25, 2000, considered here.

5. Results and Discussion

Figure 2 presents simultaneous images of the OI 777.4 nm and OI 630.0 nm emissions showing airglow depletion bands, quasi north-south aligned with the magnetic field lines.

The OI 630.0 nm emission image shows the occurrence of two main plasma bubbles in the center of the image and a few others to the right. These are well-known image patterns of the OI 630.0 nm emission, which were used in the past to study the morphology, dynamics, seasonal variation, and solar cycle effects of large-scale ionospheric irregularities, ionospheric behavior during geomagnetic storms, and ionospheric plasma drift dynamics.

The OI 777.4 nm emission image, presented in the left panel of Figure 2, shows in great detail the fine structure (with sharp longitudinal gradients) of the quasi field-aligned ionospheric plasma bubbles, which are not seen in the OI 630.0 nm emission image. These bubble structures are closely spaced in longitude, so that their internal densities seem to be influenced by their local electric fields and local ionospheric conditions. It should be pointed out that high-resolution Atmospheric Explorer E (AE-E) satellite (low-inclination orbit at ~ 400 km permitted east-west measurements of plasma bubbles) plasma density measurements show that irregularities have the form of sharp quasiperiodic depletions [*Tsunoda et al.*, 1982; *Basu et al.*, 1983; *Hysell and Kelley*, 1997], which are consistent with our present OI 777.4 nm imaging observations.

The airglow signatures of depleted flux tubes, associated with equatorial spread *F* (ESF) plumes at the equator, have been studied in the past using OI 630.0 nm images [*Weber et al.*, 1978; *Mendillo and Baumgardner*, 1982; *Anderson and Mendillo*, 1983; *Malcolm et al.*, 1984; *Sahai et al.*, 1994, 1998, 1999; *Mendillo et al.*, 1997; *Bittencourt et al.*, 1997; *Fagundes et al.*, 1997, 1999], OI 777.4 nm images, and conventional photometers [*Moore and Weber*, 1981; *Sahai et al.*, 1981; *Bittencourt et al.*, 1983; *Mendillo et al.*, 1985; *Rohrbaugh et al.*, 1989; *Tinsley et al.*, 1997]. It appears that the previous detected images did not have sufficiently high resolution to show the fine structure and the ray-like longitudinal pattern that our OI 777.4 nm images are revealing now for the first time. The OI 777.4 nm emission image, shown in Figure 2, presents a detailed ray-like

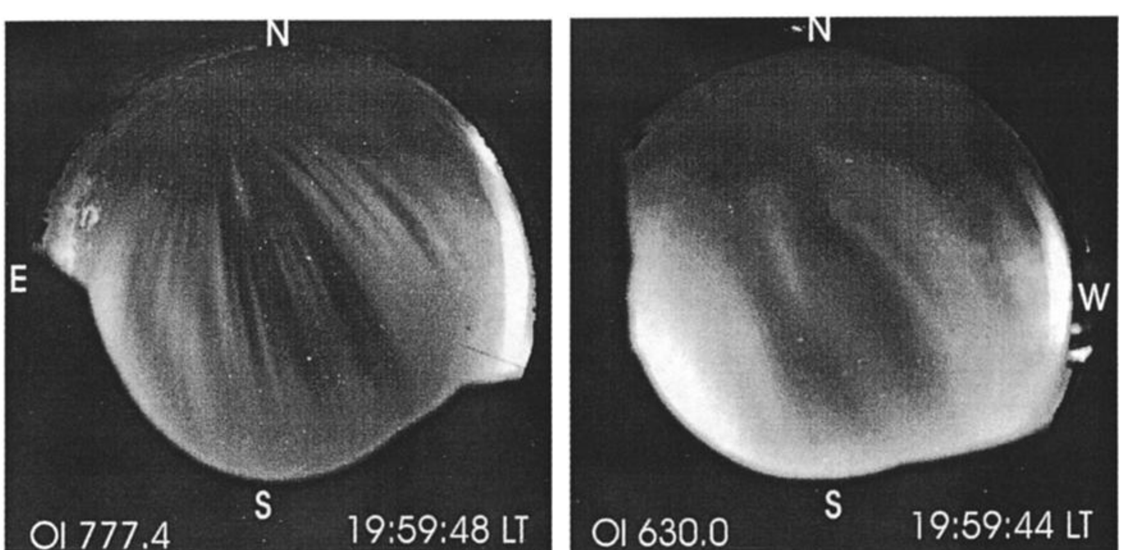

Figure 2. All-sky imaging system data obtained on the night October 23, 2000, at 1959:48 and 1959:44 LT showing the presence of large-scale ionospheric plasma irregularities for the atomic oxygen emission (left) OI 777.4 nm emission and (right) OI 630.*0* nm emission. The OI 777.4 nm image shows a ray-like fine structure pattern, associated with the quasi field-aligned irregularities, which is not observed through the OI 630.0 nm emission.

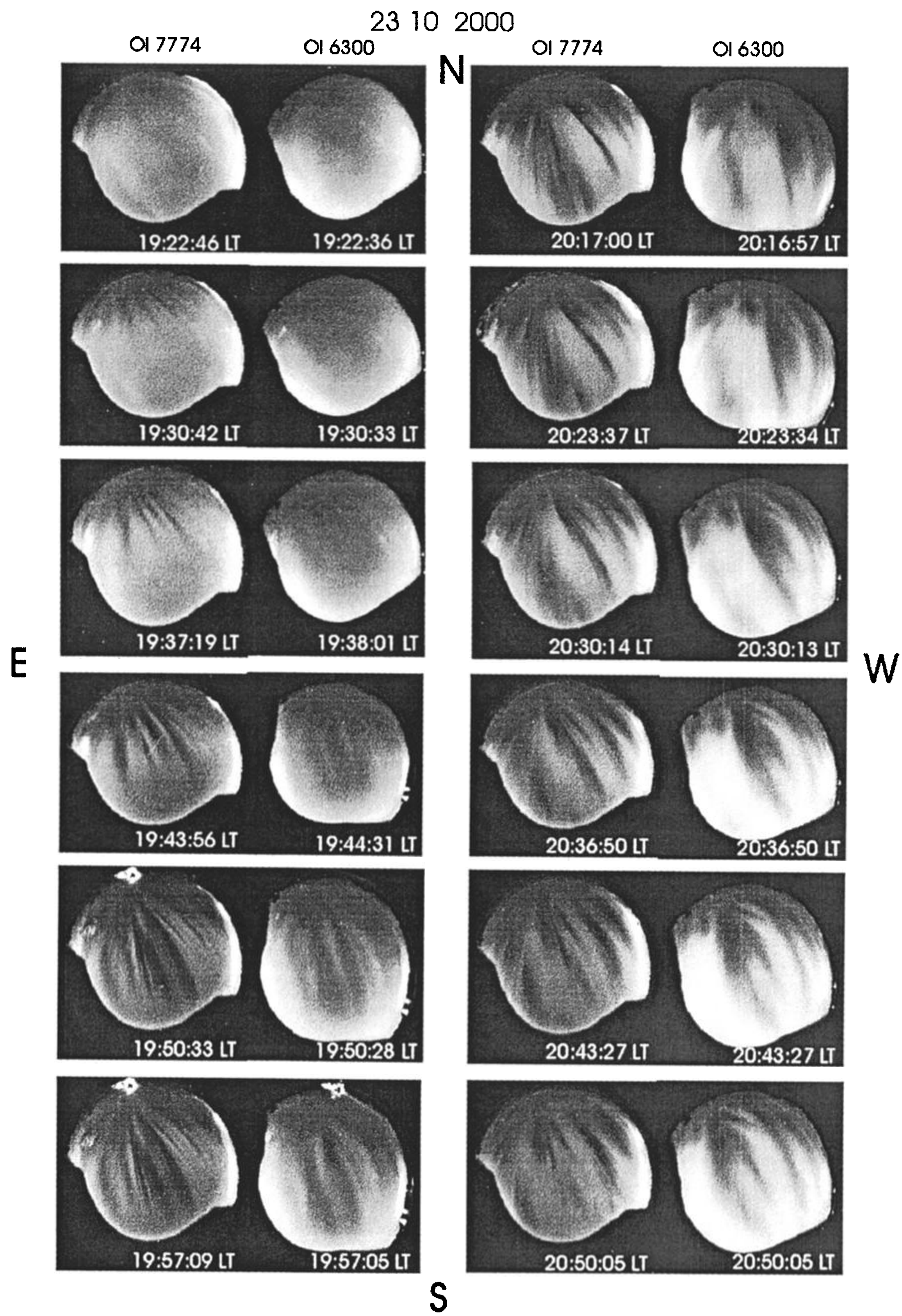

Figure 3. Two sequences of all-sky airglow images showing the time evolution and spatial characteristics of ionospheric plasma irregularity events for the OI 777.4 nm and OI 630.0 nm emissions. Note the great difference in the spatial structure of the irregularities as seen through each emission.

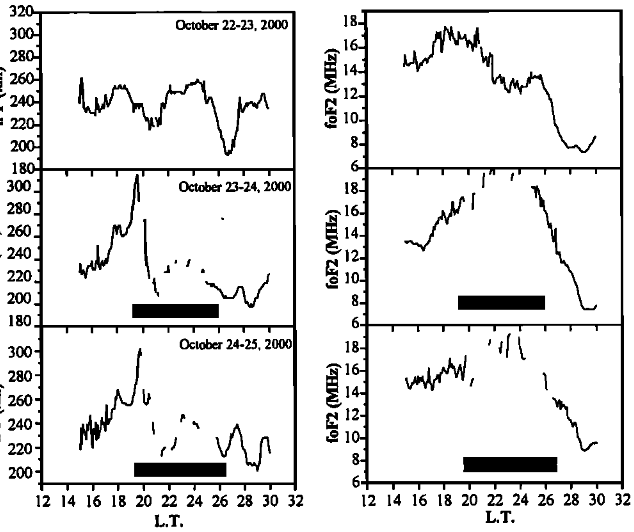

Figure 4. Local time variation of the ionospheric parameters f_0F_2 and $h'F$ obtained at a low-latitude station (São José dos Campos) on the nights of October 22-23, 23-24, and 24-25, 2000. Thick horizontal lines indicate the periods when range spread F signatures were seen on the ionograms.

structure pattern, associated with the quasi field-aligned bubbles, which are not seen in the simultaneous OI 630.0 nm emission image. The OI 777.4-nm emission is prompt, in comparison to the 110-s lifetime of the metastable $O(^1D)$ state that gives rise to the OI 630.0 nm emission. Thus the OI 777.4 nm emission images are not subject to the blurring effect [*Tinsley*, 1982], with a scale size of a few kilometers, that is present in the OI 630.0 nm images. This is because of the effect of diffusion of the metastable atoms, leading to a much less defined depletion structure. These detailed structures, seen through the OI 777.4 nm emission, have not been reported before.

Another important difference in the optical signatures of ionospheric plasma bubbles, as seen from these two atomic oxygen emissions, is that they are produced in different height regions of the ionosphere. While the OI 630.0 nm emission comes from a somewhat narrow height region, with its volume emission rate peak about one scale height below the F_2 peak (and its intensity shows a strong inverse dependence on the ionospheric vertical motions), the OI 777.4 nm emission comes from the whole ionosphere with its volume emission rate peak almost coincident with the F_2 peak (and its intensity does not depend on the ionospheric vertical motions but only on the ionospheric density and profile shape).

Figure 3 shows two simultaneous sequences of images for the OI 777.4 nm and OI 630.0 nm emissions, for the period 1922-2050 LT. Through these images we can see that the airglow depletion bands appear first in the OI 777.4 nm emission (1930:42 LT) and that only after ~ 15 min they are observed in the OI 630.0 nm emission (1944:31 LT). This earlier appearance was also illustrated by *Tinsley et al.* [1997] and it is due to the fact that the seeding and onset of ionospheric plasma irregularities seem to occur when the bottomside of the ionospheric layer is above 300 km. In the sequence of images shown in Figure 3 we can observe the striking differences in the ionospheric plasma bubble structures revealed by these two emissions, in which highly structured, quasi field-aligned ray-like patterns are seen through the OI 777.4 nm emission. The plasma bubble structures, observed from both the emissions, show an eastward drift.

Figure 4 presents the local time variation of the ionospheric parameters $h'F$, f_0F_2 and range spread F for October 22-23, 23-24, and 24-25, 2000. One of the important factors for plasma bubble formation is known to be a rapid upward lifting of the F layer just after sunset. Notice that on October 22-23 there was no upward lifting of the F layer (and no spread F), and no plasma bubbles were observed, whereas on the night of October 23-24 there was a rapid upward motion of the ionosphere just after sunset (~ 1900 LT), with the onset of ionospheric irregularities. The night of October 22-23 was magnetically disturbed.

6. Summary and Conclusions

Ground-based observations of the OI 630.0 nm and OI 777.4 nm emissions, using all-sky imaging systems, together with local ionospheric parameters measured with an ionosonde, have been carried out at a low-latitude station in Brazil. This study concentrated mainly on the high-resolution structures revealed by the OI 777.4 nm emission images during the occurrence of large-scale ionospheric irregularities. The main findings can be summarized as follows.

1. A new well-defined, ray-like structure, with sharp longitudinal gradients, has been revealed by the high-resolution OI 777.4 nm images, as the optical manifestation of ionospheric plasma bubbles. These well-defined structures are not observed in the OI 630.0 nm images. Since the OI 777.4 nm emission is prompt, in comparison to the 110-s lifetime of the metastable $O(1D)$ state, which is the origin of the OI 630.0 nm emission, the images recorded from the OI 777.4 nm emission are sharper than the corresponding OI 630.0 nm images. Also, they are more closely related to the associated ionospheric plasma phenomena.

2. The OI 777.4 nm images show plasma bubble formation at an earlier evening time (~ 15 min) as compared with the OI 630.0 nm images. The main reason for this feature is the high dependence that the OI 630.0 nm emission intensities have with respect to the F layer height. It is well known that the generation of plasma bubbles is strongly connected to a rapid upward lifting of the F layer at evening hours and that when the layer is at high altitudes, the OI 630.0 nm intensities become weak. On the other hand, the OI 777.4 nm intensities have no height dependence but a strong dependence on the ionospheric electron concentrations.

Acknowledgments. Partial funding for this work was provided through the Fundação de Amparo à Pesquisa do Estado de São Paulo (FAPESP), 98/09892-0 and 98/12493-0, Conselho Nacional de Desenvolvimento Científico e Tecnológico (CNPq), 521243/97-1 and 301630/88-7, and Fundação Vale Paraibana de Ensino (FVE), Brazil.

Janet G. Luhmann thanks Joel D. Burcham and another referee for their assistance in evaluating this paper.

References

Anderson, D. N., and M. Mendillo, Ionospheric conditions affecting the evolution of equatorial plasma depletions, *Geophys. Res. Lett.*, *10*(7), 541-544, 1983.

Basu, S., S. Basu, J. P. McClure, W. B. Hanson, and H. E. Whitney, High resolution topside in situ data of electron densities and VHF/GHz scintillations in the equatorial region, *J. Geophys. Res.*, *88*(A1), 403-415, 1983.

Bittencourt, J. A., N. R. Teixeira, Y. Sahai, and H. Takahashi, Mapping of Ionospheric *F*-region parameters from atomic oxygen airglow emissions, *J. Atmos. Terr. Phys.*, *45*(10), 697-705, 1983.

Bittencourt, J. A., Y. Sahai, P. R. Fagundes, and H. Takahashi, Simultaneous observations of equatorial *F*-region plasma depletions and thermospheric winds, *J. Atmos. Terr. Phys.*, *59*(9), 1049-1059, 1997.

Fagundes, P. R., Y. Sahai, I. S. Batista, J. A. Bittencourt, M. A. Abdu, and H. Takahashi, Vertical and zonal equatorial *F*-region plasma bubble velocities determined from OI 630 nm nightglow imaging, *Adv. Space Res.*, *20*(6), 1297-1300, 1997.

Fagundes, P. R., Y. Sahai, I. S. Batista, M. A. Abdu, J. A. Bittencourt, and H. Takahashi, Observations of day-to-day variability in precursor signatures to equatorial *F*-region plasma depletions, *Ann. Geophys.*, *17*, 1053-1063, 1999.

Garcia, F. J., M. J. Taylor, and M. C. Kelley, Two-dimensional spectral analysis of mesospheric airglow image data, *Appl. Opt.*, *36*(29), 7374-7385, 1997.

Hysell, D. L., and M. C. Kelley, Decaying equatorial *F* region plasma depletions, *J. Geophys. Res.*, *102*(A9), 20,007-20,017, 1997.

Kelley, M. C., Equatorial spread-F: Recent results and outstanding problems, *J. Atmos. Terr. Phys.*, *47*(8-10), 745-752, 1985.

MacDougall, J. W., G. E. Halland, and K. Hayashi, *F* region gravity waves in the central polar cap, *J. Geophys. Res.*, *102*(A7), 14,513-14,530, 1997.

Malcolm, R., C. Miles, and B. A. Tinsley, Field-aligned observation of trans-equatorial bubbles from Rarotonga in 1969-70, *Geophys. Res. Lett.*, *11*(7), 665-668, 1984.

Mendillo, M., and J. Baumgardner, Airglow characteristics of equatorial plasma depletions, *J. Geophys. Res.*, *87*(A9), 7641-7652, 1982.

Mendillo, M., H. Spence, and S. T. Zalesak, Simulation studies of ionospheric airglow signatures of plasma depletions at the equator, *J. Atmos. Terr. Phys.*, *47*(8), 885-893, 1985.

Mendillo, M., J. Baumgardner, X.-Q. Pi, P. J. Sultan, and R. Tsunoda, Onset conditions for equatorial spread-F, J. *Geophys. Res.*, *97*(A9), 13,865-13,876, 1992.

Mendillo, M., J. Baumgardner, M. Colerico, and D. Nottingham, Imaging science contributions to equatorial aeronomy: Initial results from the MISETA program, *J. Atmos. Terr. Phys.*, *59*(13), 1587-1599, 1997.

Moore, J. G., and E. J. Weber, OI 6300 and 7774 A airglow measurements of equatorial plasma depletions, *J. Atmos. Terr. Phys.*, *43*(8), 851-858, 1981.

Ossakow, S. L., Spread *F* theories: A review, *J. Atmos. Terr. Phys.*, *43*(5-6), 437-452, 1981.

Rohrbaugh, R. P., W. B. Hanson, B. A. Tinsley, B. L. Cragin, J. P. McClure, and A. L. Broadfoot, Images of transequatorial bubbles based on field-aligned airglow observations from Haleakata in 1984-1986, *J. Geophys. Res.*, *94*(A6), 6763-6770, 1989.

Sahai, Y., J. A. Bittencourt, N. R. Teixeira, and H. Takahashi, Plasma irregularities in the tropical *F*-region detected by OI 7774 A and 6300 A nightglow measurements, *J. Geophys. Res.*, *86*(A5), 3496-3500, 1981.

Sahai, Y., J. Aarons, M. Mendillo, J. Baumgardner, J. A. Bittencour, and H. Takahashi, OI 630 nm imaging observations of the equatorial plasma depletions at 16°S dip latitude, *J. Atmos. Terr. Phys.*, *56*(11), 1461-1475, 1994.

Sahai, Y., P. R. Fagundes, J. A. Bittencourt, and M. A. Abdu, Occurrence of large scale equatorial F-region plasma depletions during geo-magnetic disturbances, *J. Atmos. Terr. Phys.*, *60*(16), 1593-1604, 1998.

Sahai, Y., P. R. Fagundes, and J. A. Bittencourt, Solar cycle effects on large scale equatorial F-region plasma depletions, Adv. Space Res., *24*(11), 1477-1480, 1999.

Sahai, Y., P. R. Fagundes, and J. A. Bittencourt, Transequatorial *F*-region ionospheric plasma bubbles: Solar cycle effects, *J. Atmos. Terr. Phys.*, *62*(15), 1377-1383, 2000.

Sinha, H. S. S., and S. Raizada, Some new features of ionospheric plasma depletions over the Indian zone using all sky optical imaging, *Earth Planet. Space, 52*, 540-559, 2000.

Tinsley, B. A., Field aligned airglow observations of transequatorial bubbles in the tropical *F*-region, *J. Atmos. Terr. Phys.*, *44*(6), 547-557, 1982.

Tinsley, B. A., and J. A. Bittencourt, Determination of *F* region height and peak electron density at night using airglow emissions from atomic oxygen, *J. Geophys. Res.*, *80*(16), 2333-2337, 1975.

Tinsley, B. A., R. P. Rohrbaugh, W. B. Hanson, and A. L. Broadfoot, Images of trans-equatorial F region bubbles in 630- and 777-nm emissions compared with satellite measurements, *J. Geophys. Res.*, *102*(A2), 2057-2077, 1997.

Tsunoda, R. T., R. C. Livingston, J. P. McClure, and W. B. Hanson, Equatorial plasma bubbles: Vertically elongated wedges from the bottomside *F* layer, *J. Geophys. Res.*, *87*(A11), 9171-9180, 1982.

Weber, E. J., J. Buchau, R. Eather, and S. B. Mende, North-south aligned equatorial airglow depletions, *J. Geophys. Res.*, *83*(A2), 712-716, 1978.

J. R. Abalde and P. R. Fagundes, Laboratório de Física Atmosférica e Aeronomia , Instituto de Pesquisas e Desenvolvimento, Universidade do Vale do Paraíba, Av. Shishima Hifumi 2911, Urbanova, 12224-000 São José dos Campos, SP, Brazil. (abalde@univap.br)

J. A. Bittencourt and Y. Sahai, Instituto Nacional de Pesquisas Espaciais, Cx. Postal 515, 12201-970 São José dos Campos, SP, Brazil.

(Received February 13, 2001; revised March 20, 2001; accepted April 11, 2001.)